Available online at www.sciencedirect.com
ScienceDirect
Biomaterials 29 (2008) 1630–1637
Biomaterials
www.elsevier.com/locate/biomaterials

Preparation and rheological characterization of a gel form of the porcine urinary bladder matrix

Donald O. Freytes [a,e], Jeffrey Martin [b], Sachin S. Velankar [b], Annie S. Lee [c], Stephen F. Badylak [a,d,e,*]

[a] University of Pittsburgh, Department of Bioengineering, Pittsburgh, PA 15219, USA
[b] University of Pittsburgh, Department of Chemical Engineering, Pittsburgh, PA 15219, USA
[c] University of Pittsburgh Medical School, Department of Otolaryngology, Pittsburgh, PA 15219, USA
[d] University of Pittsburgh Medical School, Department of Surgery, Pittsburgh, PA 15219, USA
[e] McGowan Institute for Regenerative Medicine, Pittsburgh, PA 15219, USA

Received 24 July 2007; accepted 15 December 2007
Available online 16 January 2008

Abstract

Biologic scaffolds composed of extracellular matrix (ECM) have been used to facilitate the repair and reconstruction of a variety of tissues in clinical and pre-clinical studies. The clinical utility of such scaffolds can be limited by the geometric and mechanical properties of the tissue or organ from which the ECM is harvested. An injectable gel form of ECM could potentially conform to any three-dimensional shape and could be delivered to sites of interest by minimally invasive techniques. The objectives of the present study were to prepare a gel form of ECM harvested from the urinary bladder (urinary bladder matrix or UBM), to characterize the rheological properties of the gel, and finally to evaluate the ability of the gel to support *in vitro* growth of smooth muscle cells. Following enzymatic solubilization with pepsin, UBM was induced to self-assemble into a gel when brought to physiological conditions. The UBM gel supported the adhesion and growth of rat aortic smooth muscle cells when cultured under static *in vitro* conditions. The present study showed that an intact form of UBM can be successfully solubilized without purification steps and induced to repolymerize into a gel form of the UBM biologic scaffold material.

Keywords: Extracellular matrix; Viscoelasticity; Rheology; Scaffold; Gel

1. Introduction

Biologic scaffolds composed of extracellular matrix (ECM) have been used for the repair of a variety of tissues including the lower urinary tract [1,2], esophagus [3,4], myocardium [5–7], and musculotendinous [8–10] tissues, often leading to tissue-specific constructive remodeling with minimal or no scar tissue formation. These biologic scaffolds are typically prepared by decellularization of intact tissues or organs. The resulting ECM scaffold materials are composed of the structural and functional molecules that characterize the native tissue ECM such as collagen, laminin, fibronectin, growth factors, glycosaminoglycans, glycoproteins, and proteoglycans [11–13]. However, the resulting decellularized ECM is usually characterized by a two-dimensional sheet with limited ability to conform to irregular three-dimensional shapes and sizes. Therefore, the clinical utility of an ECM biologic scaffold for many clinical applications is typically restricted to topical administration or to invasive surgical procedures that can accommodate variations of the two-dimensional sheet forms.

An ECM scaffold derived from the porcine urinary bladder, referred to as urinary bladder matrix (UBM), has been previously investigated in pre-clinical studies as a biologic scaffold for the reconstruction of damaged laryngeal tissue [14], for the

* Corresponding author. McGowan Institute for Regenerative Medicine, 100 Technology Drive, Suite 200, Pittsburgh, PA 15219, USA. Tel.: +1 412 235 5148; fax: +1 412 235 5110.
E-mail address: badylaks@upmc.edu (S.F. Badylak).

0142-9612/$ - see front matter © 2007 Elsevier Ltd. All rights reserved.
doi:10.1016/j.biomaterials.2007.12.014

reconstruction of esophageal tissue [4,15], as a treatment for urinary incontinence [2], and as a myocardial patch [6,7,16] with promising results. Suspensions made from a particulate (powdered) form of lyophilized UBM have been successfully used as an injectable scaffold for the treatment of urinary incontinence in pre-clinical studies [2] but the needle size required to accommodate the particle size was prohibitive for most clinical applications, and substances such as glycerin were required to increase the viscosity of the solution.

A soluble form that can be induced to polymerize into a gel form could expand the clinical utility of ECM biologic scaffolds. ECM gels with appropriate viscosities could be delivered via minimally invasive surgical techniques with the ability to conform to three-dimensional spaces after injection. Ideally this soluble form would retain the bioactivity of the ECM scaffold and its preparation would minimize or avoid purification steps that could remove growth factors and low molecular weight peptides present in the native ECM. Previous studies have described a gel form of an ECM derived from the small intestine but the preparation required an aggressive purification process that may have resulted in the loss of bioactive molecules, and the rheological properties of the gel were not determined [17]. Gels have been formed from individual components of the ECM such as collagen and from the secreted products of cell lines (Matrigel™). Matrigel™ is not used therapeutically due to its source (tumor cell line), and individual ECM components lack the bioactivity found in minimally processed ECM scaffolds in which structural and functional molecules are present in physiologically relevant amounts.

The long-term objective of this work is to develop a gel form of the UBM scaffold that retains the bioactivity and ability to promote constructive tissue remodeling; properties that are characteristic of the 2-D sheet form of UBM. The present study is the first step towards this goal and describes a method to solubilize UBM without purification steps and a method to repolymerize the soluble UBM–ECM under physiological conditions. The present study characterizes the gelation kinetics, the rheological properties, and the static *in vitro* cytocompatibility of the UBM gel.

2. Materials and method

2.1. ECM preparation

The preparation of UBM has been previously described [20,21]. In brief, porcine urinary bladders were harvested from 6-month-old 108–118 kg pigs (Thoma Meat Market) immediately following euthanasia. The excess connective tissue and residual urine were removed. The tunica serosa, tunica muscularis externa, the tunica submucosa, and majority of the tunica muscularis mucosa were mechanically removed. The urothelial cells of the tunica mucosa were dissociated from the luminal surface by soaking the tissue in 1.0 N saline solution. The resulting biomaterial, which was composed of the basement membrane of the urothelial cells plus the subjacent lamina propria, was referred to as urinary bladder matrix (UBM). UBM sheets were placed in a solution containing 0.1% (v/v) peracetic acid (Sigma), 4% (v/v) ethanol (Sigma), and 95.9% (v/v) sterile water for 2 h. Peracetic acid residue was then removed with two 15-min phosphate-buffered saline (pH = 7.4) washes, followed by two washes with sterile water for 15 min each. The decellularized UBM sheets were then lyophilized using an FTS Systems Bulk Freeze Dryer Model 8-54 and comminuted to a particulate form using a Wiley Mini Mill (Fig. 1A).

2.2. ECM digestion and solubilization

One gram of lyophilized UBM powder (Fig. 1A) and 100 mg of pepsin (Sigma, ~2000–2300 U/mg) were mixed in 100 ml of 0.01 M HCl and kept at a constant stir for ~48 h at room temperature (25 °C). The resultant viscous solution of digested UBM or pre-gel solution had a pH of approximately 3.0–4.0 (Fig. 1B). The activity of pepsin was irreversibly inactivated when the pH was raised to 7.4 (see Section 2.4).

2.3. Gel characterization

UBM and rat-tail collagen type I (BD, Biosciences) solutions were electrophoresed on 7.5% polyacrylamide gels under reducing conditions (5% 2-mercaptoethanol). The proteins were visualized with Gel-Code Blue (Bio-Rad), and images recorded by a Kodak imaging station.

Collagen and sulfated glycosaminoglycan (S-GAG) content of the UBM gel were determined using the hydroxyproline assay [18] and the Blyscan™ assay kit (Biocolor), respectively. The Blyscan™ assay was performed according to the manufacturer's instructions. The hydroxyproline content was determined by hydrolyzing the samples with 2 M NaOH (100 μl total volume) in an autoclave at 120 °C for 20 min. The samples were neutralized with 50 μl of 4 M HCl and reacted with 300 μl of 0.056 M chloramine-T (Spectrum), mixed gently, and allowed to oxidize for 25 min at room temperature. The samples were then mixed with 300 μl of 1 M Ehrlich's aldehyde (Spectrum) and incubated at 65 °C for 20 min. A standard curve was generated using rat-tail collagen type I (BD, Biosciences) and used to calculate the total amount of collagen present in the digested UBM solutions. The colorimetric change was determined by the absorbance at 550 nm using a SpectraMax spectrophotometer (Molecular Devices). Three different batches of UBM were tested ($n = 3$).

2.4. Gelation

UBM and rat-tail collagen type I gels were formed by mixing 0.1 N NaOH (1/10 of the volume of pre-gel solution) and 10× PBS pH 7.4 (1/9 of the volume of pre-gel solution) at 4 °C. The solution was brought to the desired volume/concentration using cold (4 °C) 1× PBS pH 7.4 and placed at 37 °C for gelation to occur. Collagen and UBM gels are shown in Fig. 1C.

Turbidimetric gelation kinetics was determined spectrophotometrically as previously described [19]. Final gel solutions were kept at 4 °C and transferred to a cold 96-well plate by placing 100 μl/well in triplicate. The SpectraMax spectrophotometer (Molecular Devices) was pre-heated to 37 °C, the plate placed in the spectrophotometer, and the turbidity of each well was measured at 405 nm every 2 min for 1.5 h. The absorbance values for each well were recorded and averaged. Three individual tests were performed on the same batch of collagen type I ($n = 3$) and five ($n = 5$) individual tests were performed on different batches of the UBM gel. Each individual test was conducted in triplicates and averaged. The time needed to reach 50% of the maximum turbidity measurement (e.g. maximum absorbance value) was defined as $t_{1/2}$ and the lag phase (t_{lag}) was calculated by extrapolating the linear portion of the curve (see Fig. 5B). The speed (S) of the gelation based on turbidimetric measurements was determined by calculating the maximum slope of the growth portion of the curve as shown in Fig. 5B.

2.5. Rheological measurements

The sample was subjected to an oscillatory strain of

$$\gamma(t) = \gamma_0 \cos(2\pi f t) \quad (1)$$

where γ_0 was the amplitude of the sinusoidal strain, t was the time, and f was the frequency. The sample developed a sinusoidal stress described as follows:

$$\sigma(t) = |G^*|\gamma(t) \quad (2)$$

where G^* was the frequency dependent complex modulus of the sample. The real part of G^*, denoted G', was in phase with the applied strain and was called the storage modulus since it corresponded to storage of mechanical energy in

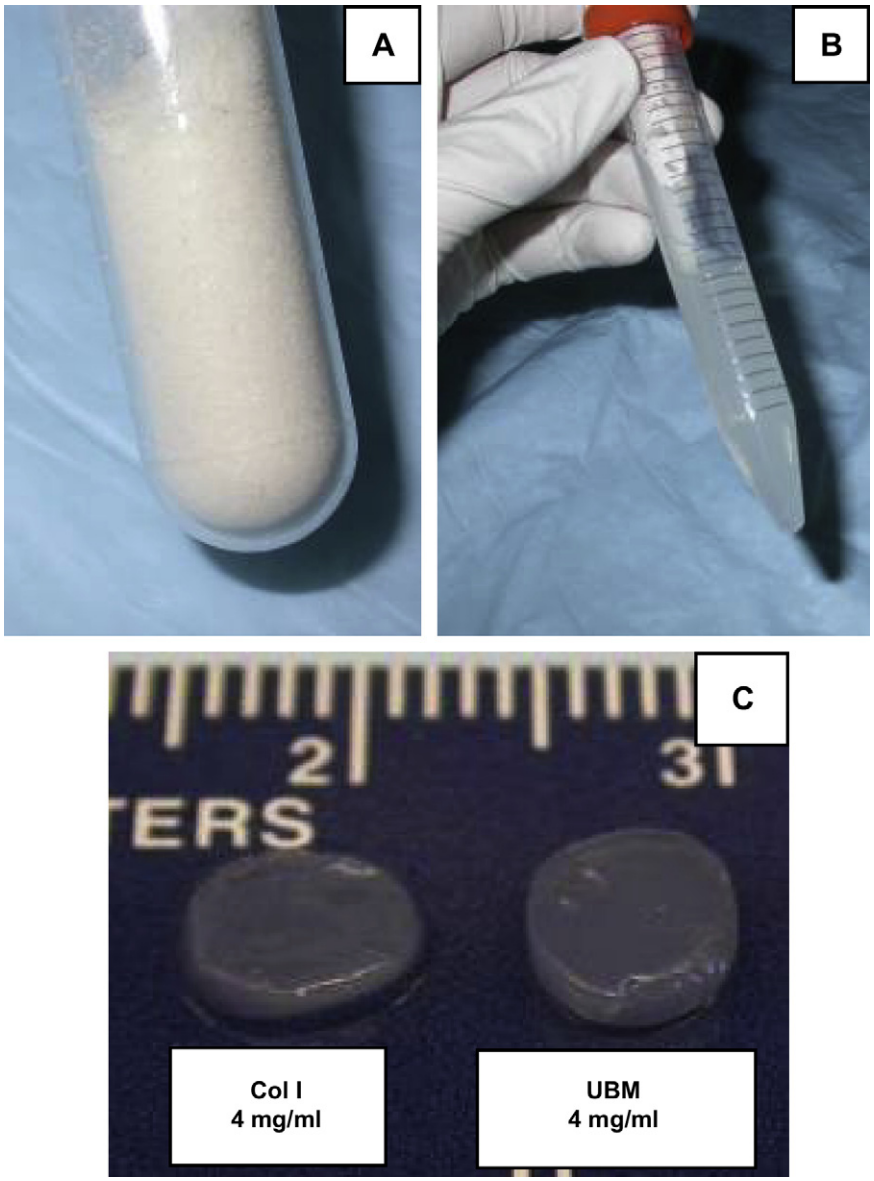

Fig. 1. (A) Lyophilized UBM powder; (B) pepsin digested UBM at a concentration of 10 mg/ml; (C) collagen type I and UBM gels.

the elastic deformation of the sample. The imaginary portion of G^*, denoted G'', was 90° out of phase with the applied strain and was called the loss modulus since it corresponded to the loss of energy by viscous dissipation within the sample. Since the sample was expected to develop solid-like characteristics as gelation proceeds, G' was expected to increase significantly.

A final property of interest was the magnitude of the complex viscosity defined as follows:

$$|\eta^*| = \frac{|G^*|}{2\pi f} = \frac{\sqrt{G'^2 + G''^2}}{2\pi f} \tag{3}$$

where $|\eta^*|$ was the frequency dependent complex viscosity, G^* was the frequency dependent complex modulus, and f was the frequency. It is common to fit complex viscosity vs frequency data to a power-law of the form:

$$\left|\eta^*\right| = kf^{-n} \tag{4}$$

where k and n are both constants.

Rheological experiments were performed with a TA Instruments AR2000 stress-controlled rheometer using a 40-mm diameter parallel plate geometry and a Peltier cell to maintain the sample temperature. The samples were prepared as discussed earlier and loaded into the rheometer with the Peltier cell maintaining a temperature of 15 °C. The sample edge was protected from evaporation by applying mineral oil. The temperature was then set to 37 °C to induce gelation; the Peltier cell typically reached a temperature of 30 °C within 10 s and 37 °C within 50 s. During this increase in temperature and the subsequent gelation, the oscillatory moduli of the sample were monitored continuously at a fixed frequency of 0.159 Hz (1 rad/s) and a strain of 5%. When there was no further change in the elastic modulus (G') with time, gelation was deemed to be complete. The final linear viscoelastic properties of the gel were measured by performing a frequency sweep between 15.9 Hz (100 rad/s) and 0.08 Hz (0.5 rad/s) at 37 °C and 5% strain and fitted to Eq. (4). Three samples from different batches of digested UBM were tested for each gel configuration ($n = 3$). The same batch of collagen type I was tested.

2.6. Cell proliferation assays

Vascular smooth muscle cells (rSMCs) were harvested as previously described from rat aortas [20] and expanded in DMEM with low bicarbonate and supplemented with 10% fetal bovine serum (FBS) and 100 U/ml

Penicillin/100 μg/ml Streptomycin. The 48-h proliferation of rSMCs was measured by seeding the surface of 6-mm disks of lyophilized UBM, collagen type I, and UBM gels in triplicate. The collagen and UBM gels were prepared by adding 100 μl of the gel (3 mg/ml) into wells of 96-well plates. rSMCs were seeded onto the surface of the gels and the 6-mm lyophilized UBM disks at a density of 2×10^4 cells/well. A well with a 6-mm lyophilized UBM disk and wells with each type of gel incubated with media without cells served as controls. After 48 h in culture, non-adherent cells were aspirated and the activity of the attached cells was quantified using the MTT assay (Sigma). Three different batches of UBM were tested ($n = 3$).

Growth of rSMCs on UBM gels was also evaluated by histological methods. Disks of UBM gel were made using a stainless steel ring (1.5 cm in diameter) as a mold. rSMCs were seeded on the top surface of the gel at a density of 0.5×10^6 cells/cm^2. Medium was changed every other day and the cells were allowed to grow for 10 days. The samples were then fixed with 10% buffered formalin and sections stained using Masson's Trichrome stain.

2.7. Scanning electron microscopy

The surface morphology of the UBM gels was examined using scanning electron microscopy (SEM). The specimens were fixed in cold 2.5% glutaraldehyde and rinsed in PBS, followed by a dehydration process through a graded series of ethanol (30–100%), and finally critically point dried in an Emscope CPD 750 critical point dryer. The samples were attached to aluminum SEM specimen mounting stubs (Electron Microscopy Sciences) and sputter coated with a gold palladium alloy using a Sputter Coater 108 Auto (Cressington Scientific Instruments). Finally, samples were examined using a scanning electron microscope (JEOL 6330F). Images were taken at a 5000 and 10,000× magnification.

2.8. Statistical analysis

A one-sided *t*-test was used to determine significant differences between mean values of the gelation constants and the proliferation values ($p < 0.05$). The linear relationship between complex viscosity and frequency was determined using a least square fit method.

3. Results

3.1. UBM gel characterization

The collagen concentration for pepsin digested UBM was 0.8 ± 0.2 mg/mg of dry lyophilized UBM powder (mean ± SD). The total S-GAG content was 7.6 ± 2.8 μg/mg of dry lyophilized UBM powder (mean ± SD). The electrophoresed solutions of UBM and purified collagen type I showed bands at similar locations confirming a large collagen type I component of UBM. UBM showed additional protein bands that were distinct from the purified collagen type I as shown in Fig. 2. Scanning electron microscopy showed a fibrillar appearance of the UBM gels at concentrations of 3 mg/ml and 6 mg/ml (Fig. 3A–D).

3.2. In vitro cell adhesion and proliferation

Rat aortic smooth muscle cells were able to grow on UBM gels under static culture conditions. After 10 days in culture, rSMCs contracted the gels and formed a multilayer of cells as shown in Fig. 4A. The percentage of cellular content between the gels and the lyophilized UBM scaffold after 48 h of *in vitro* culture was greater in the UBM gels when compared to purified collagen as shown in Fig. 4B.

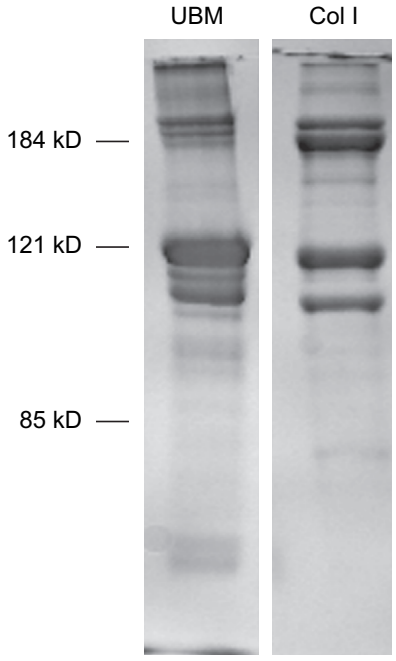

Fig. 2. Protein gel of collagen type I and UBM.

3.3. Turbidimetric gelation kinetics

The turbidimetric gelation kinetics and the calculated parameters are shown in Fig. 5 and the results presented in Table 1. The turbidimetric gelation kinetics for UBM and collagen type I gels showed a sigmoidal shape (Fig. 5A). Collagen type I gels at a concentration of 3 mg/ml became more turbid following gelation than UBM gels at a concentration of 3 mg/ml and 6 mg/ml (Fig. 5A). The lag phase (t_{lag}) and the time required to reach half the final turbidity ($t_{1/2}$) were greater in the UBM gels (at 3 mg/ml and 6 mg/ml) than collagen type I gels (3 mg/ml). In addition, the speed of the turbidimetric gelation kinetics (S) was less for UBM when compared to collagen type I. There was no change in t_{lag}, $t_{1/2}$, and S between 3 mg/ml and 6 mg/ml UBM gels. The maximum turbidity values changed with increasing UBM concentration.

3.4. Rheological properties

Both the storage modulus (G') and the loss modulus (G'') changed over time and were characterized by a sigmoidal shape after the temperature of the sample was raised from 15 °C to 37 °C as shown in Fig. 6. G' and G'' reached steady state after approximately 8–12 min suggesting that gelation had occurred. The kinetics of G' and G'' were faster than the turbidimetric kinetics. The dynamic viscosities of both UBM and collagen type I are shown in Fig. 7 over a frequency range of ~0.08–15 Hz and the results are summarized in Table 2. The value of $n \sim 1$ for both UBM and collagen type I occurs

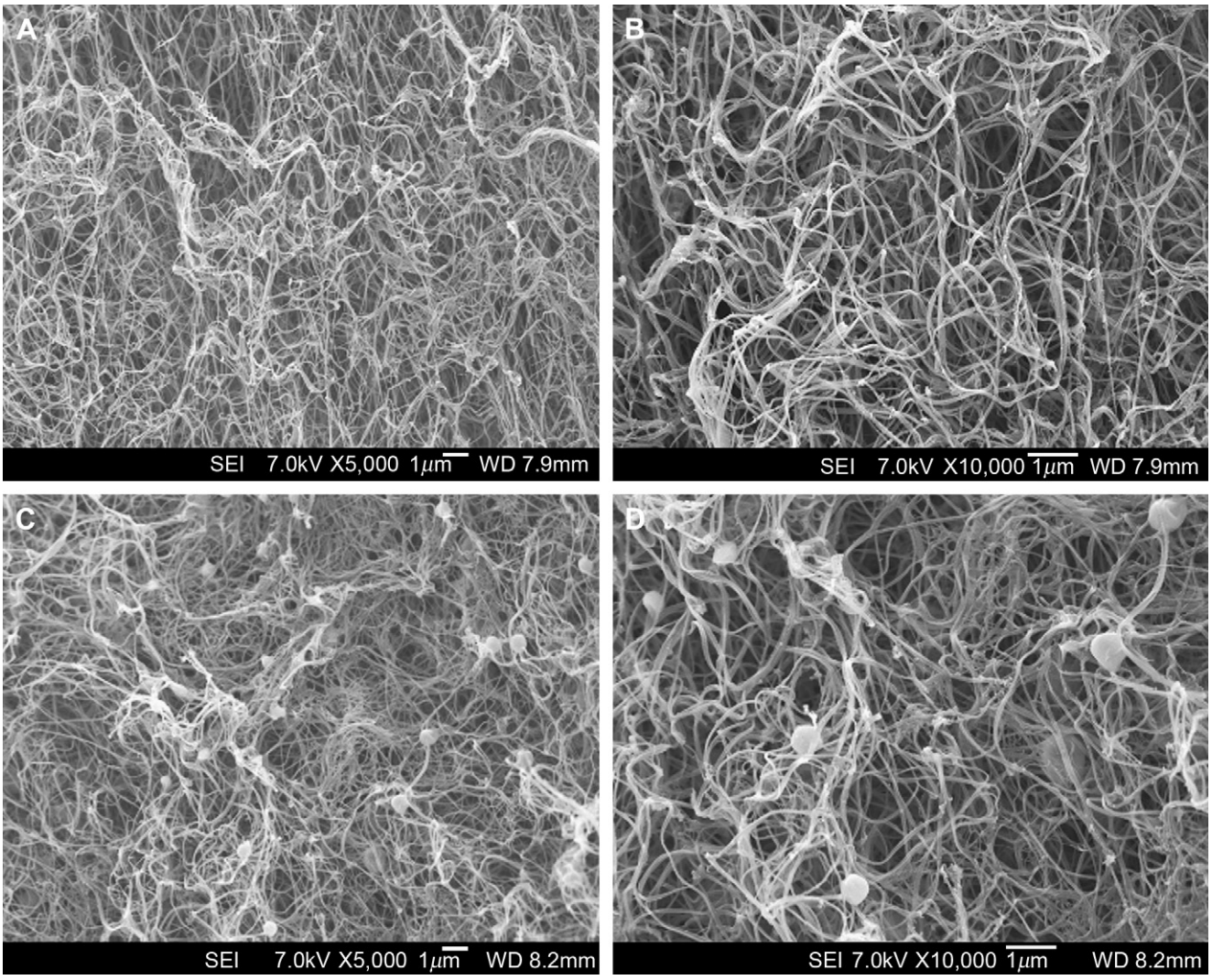

Fig. 3. Scanning electron micrograph of UBM gels: (A) 3 mg/ml at 5000×; (B) 3 mg/ml at 10,000×; (C) 6 mg/ml at 5000×; (D) 6 mg/ml at 10,000×.

because $G' \gg G''$ and G' is independent of frequency. Therefore, the complex viscosity of UBM and collagen were inversely proportional to frequency since $|\eta^*| \sim G'/(2\pi f)$.

4. Discussion

The present study characterized the gelation kinetics, rheological properties, and the cytocompatibility of a gel form of an ECM scaffold derived from the porcine urinary bladder called urinary bladder matrix. The conditions developed in the present study allowed for the digestion of the UBM scaffold without the need for purification steps that would adversely or excessively affect the molecular composition of the ECM. The digested UBM self-assembled into a gel when brought to physiological ionic strength, pH, and temperature. The gelation kinetics, rheological properties, and the ability of the gel to support smooth muscle cell growth *in vitro* were also determined.

The components responsible for the gelation of UBM are unknown but most likely gelation was due to the presence of self-assembling molecules such as collagens, laminins, and proteoglycans [21,22]. The turbidimetric gelation kinetics of UBM gels were slower than purified collagen type I at similar total protein concentrations presumably due to the presence of glycosaminoglycans in the UBM solution and/or the presence of different types of collagens or molecules such as fibronectin which are known to modulate collagen self-assembly [21–25]. The role of glycosaminoglycans in the gelation kinetics of UBM is supported by previous studies that have shown a decrease in final turbidimetric absorbance and changes in gelation kinetics of collagen type I gels when mixed with different glycosaminoglycans [24]. The exact reasons for the changes in turbidity and gelation kinetics remain unknown. However, the findings suggest that the process is not simply collagen chemistry but rather a result of the interplay of all of the components within the digested UBM.

Rat aortic smooth muscle cells (rSMCs) were able to grow upon and adhere to the UBM gels. After 48 h of incubation, greater numbers of cells were found on the lyophilized sheets of UBM when compared to collagen type I and UBM gels.

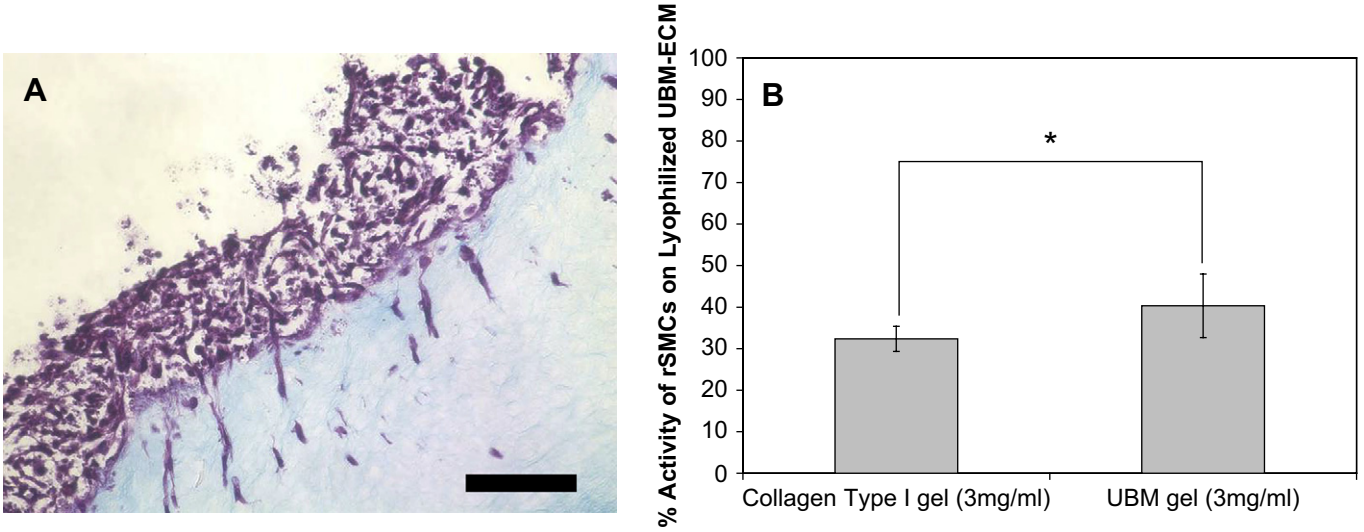

Fig. 4. (A) Rat smooth muscle cells grown on UBM gels for 10 days (scale bar = 100 μm); (B) comparison of the cellular activity of rSMCs on UBM and collagen type I gel when compared to lyophilized UBM scaffolds. Data represent mean ± SD. *$p < 0.05$ (paired one-sided t-test).

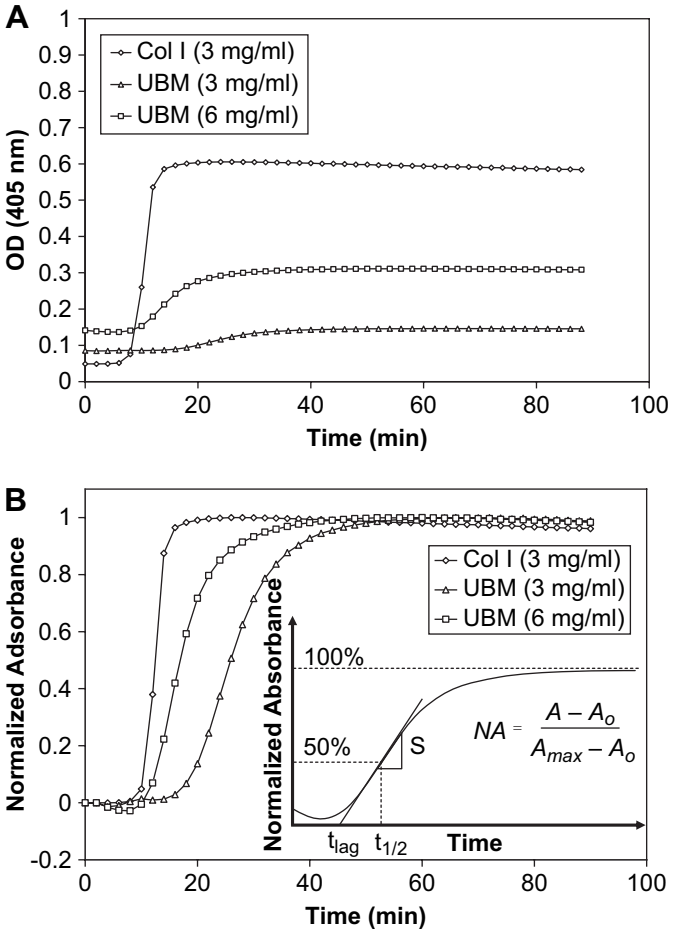

Fig. 5. (A) Turbidimetric gelation kinetics of collagen type I and UBM gels; (B) normalized turbidimetric gelation kinetics of collagen type I and UBM gels (inset: diagrammatic representation of the normalization and the parameters determined from the gelation kinetics).

The greater number of cells found on the lyophilized UBM could be due to differences in the mechanical or structural properties of the substrates (lyophilized sheet vs gel). Interactions between cells and its substrate have been known to modulate cell behavior such as adhesion, proliferation, and migration [26]. Another plausible explanation could be the presence of bioactive proteins/peptides present at the surface of the lyophilized UBM that are no longer surface-located in the gel form. If such bioactive proteins/peptides are retained during the digestion process, it could explain the higher cellular content found on UBM gels when compared to collagen type I after the 48-h incubation period. Future studies will determine the biochemical composition of the UBM gel as well as the retention of bioactivity after enzymatic digestion of UBM.

The rheological properties of the UBM gel were determined and showed that both the storage modulus (G') and the loss modulus (G'') increased as a function of time after the temperature of the buffered solution was increased to 37 °C. The gelation of UBM observed by turbidimetric and rheologic methods showed a sigmoidal shape. After approximately ~20–30 min, the turbidity and the shear moduli of UBM reached a constant value at which point gelation was deemed complete. After the gelation period, G' was greater than G'' suggesting that the gel behaved as a solid-like structure. This transition to a solid structure occurred for both 3 mg/ml and 6 mg/ml UBM gels. As seen by the changes in

Table 1
Results from the turbidimetric analysis of the UBM gelation kinetics

Material	S	$t_{1/2}$	t_{lag}
Collagen type I 3 mg/ml	0.20 (0.01)*	12.2 (1.1)*	9.7 (0.8)*
UBM 3 mg/ml	0.07 (0.01)	24.4 (2.4)	16.8 (2.0)
UBM 6 mg/ml	0.09 (0.04)	22.4 (4.9)	15.2 (3.3)

Data represent mean ± SD; *$p < 0.05$.

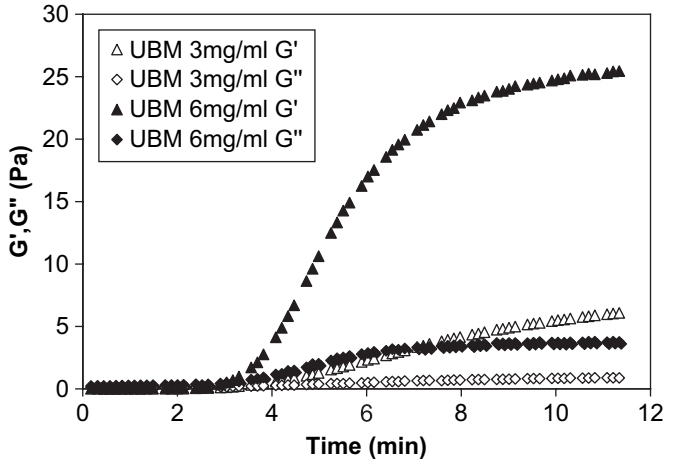

Fig. 6. Representative curves of the gelation kinetics of UBM gels determined during the mechanical testing of the gels based on the storage modulus (G') and the loss modulus (G'').

dynamic complex viscosity (η^*) and both G' and G'' as a function of concentration, the rheological properties change as a function of the final concentration. Changes in concentration can be used to tailor the rheological properties of the gel for specific applications.

The UBM gels developed in the present study have lower viscosity values than some of the injectable materials currently in clinical use [27–29]. Also, high UBM concentrations (6 mg/ml) were required to obtain gels with similar rheological properties to collagen type I gels (3 mg/ml). The increase in protein concentration needed to obtain the desired rheological properties (similar to collagen or hyaluronic acid) may affect the diffusion of oxygen, nutrients, and waste across the gel. Changes in diffusion may affect the behavior of cells if the gel is intended as a cell delivery material or if cells are embedded within the gel [30,31]. The *in vitro* response of cells when seeded within the gel as well as the host tissue response to the gel will be the subject of future studies.

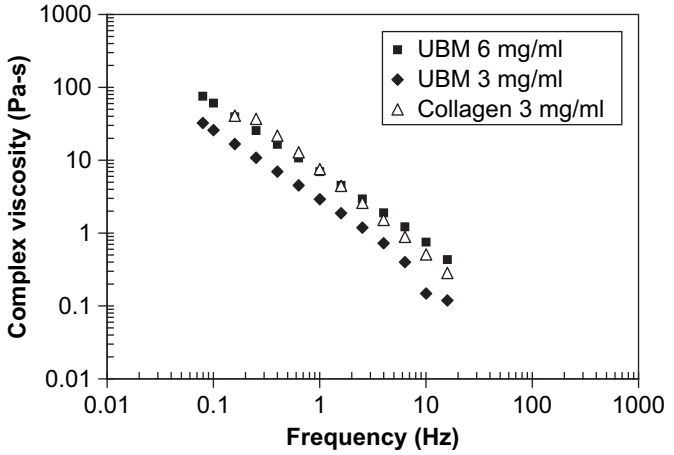

Fig. 7. Viscosity vs frequency plots of UBM gels and collagen type I gels. Data represents mean values.

Table 2
Comparison of the complex viscosity of UBM gels with commercially available injectable materials

Material	k	n	r^2	Frequency range (Hz)	Reference
Collagen type I 3 mg/ml	6.92	−1.117	0.995	0.01–15	–
Urinary bladder matrix 3 mg/ml	2.35	−1.062	0.988	0.01–15	–
Urinary bladder matrix 6 mg/ml	5.69	−0.955	0.999	0.01–15	–
Gelatin (Gelfoam)	149.39	−0.903	0.997	0.01–15	[27]
Zyplast™	99.851	−0.915	0.998	0.01–15	[27]
Zyderm™	66.395	−0.915	0.998	0.01–15	[27]
Zyderm™	12	−0.860	0.977	0.01–100	[29]
Cymetra®	19.9	−0.778	0.972	0.01–100	[29]
Hyaluronic acid-DTPH	3.19	−0.744	0.974	0.01–100	[29]
Human abdominal subcutaneous fat	23.576	−0.951	0.994	0.01–15	[27]
Polytetrafluoroethylene (PTFE)	1151.9	−1.027	0.997	0.01–15	[27]

5. Conclusions

The present study showed that UBM can be successfully solubilized and formed into a gel that can be used as an injectable scaffold for clinical applications. The present study also shows that UBM gels support the adherence and growth of rat aortic smooth muscle cells.

Acknowledgements

We would like to thank Dr. John Stankus and Dr. William Wagner for supplying the rat smooth muscle cells. We would also like to thank Dr. Ann Stewart-Akers, Dr. Julie Myers-Irvine, Colin Pesyna, Marc Rubin, Jeannie Brin and Scott Zundel for their help and assistance.

References

[1] Dedecker F, Grynberg M, Staerman F. Small intestinal submucosa (SIS): prospects in urogenital surgery. Prog Urol 2005;15(3):405–10.
[2] Wood JD, Simmons-Byrd A, Spievack AR, Badylak SF. Use of a particulate extracellular matrix bioscaffold for treatment of acquired urinary incontinence in dogs. J Am Vet Med Assoc 2005;226(7):1095–7.
[3] Badylak S, Meurling S, Chen M, Spievack A, Simmons-Byrd A. Resorbable bioscaffold for esophageal repair in a dog model. J Pediatr Surg 2000;35(7):1097–103.
[4] Badylak SF, Vorp DA, Spievack AR, Simmons-Byrd A, Hanke J, Freytes DO, et al. Esophageal reconstruction with ECM and muscle tissue in a dog model. J Surg Res 2005;128(1):87–97.
[5] Badylak S, Obermiller J, Geddes L, Matheny R. Extracellular matrix for myocardial repair. Heart Surg Forum 2003;6(2):E20–6.
[6] Badylak SF, Kochupura PV, Cohen IS, Doronin SV, Saltman AE, Gilbert TW, et al. The use of extracellular matrix as an inductive scaffold for the partial replacement of functional myocardium. Cell Transplant 2006;15(Suppl. 1):S29–40.
[7] Robinson KA, Li J, Mathison M, Redkar A, Cui J, Chronos NA, et al. Extracellular matrix scaffold for cardiac repair. Circulation 2005; 112(Suppl. 9):I135–43.
[8] Badylak S, Arnoczky S, Plouhar P, Haut R, Mendenhall V, Clarke R, et al. Naturally occurring extracellular matrix as a scaffold for musculoskeletal repair. Clin Orthop Relat Res 1999;(Suppl. 367):S333–43.

[9] Badylak SF, Tullius R, Kokini K, Shelbourne KD, Klootwyk T, Voytik SL, et al. The use of xenogeneic small intestinal submucosa as a biomaterial for Achilles tendon repair in a dog model. J Biomed Mater Res 1995;29(8):977–85.
[10] Zantop T, Gilbert TW, Yoder MC, Badylak SF. Extracellular matrix scaffolds are repopulated by bone marrow-derived cells in a mouse model of Achilles tendon reconstruction. J Orthop Res 2006;24(6):1299–309.
[11] Badylak SF. The extracellular matrix as a scaffold for tissue reconstruction. Semin Cell Dev Biol 2002;13(5):377–83.
[12] Badylak SF. Xenogeneic extracellular matrix as a scaffold for tissue reconstruction. Transpl Immunol 2004;12(3–4):367–77.
[13] Badylak SF. Regenerative medicine and developmental biology: the role of the extracellular matrix. Anat Rec B New Anat 2005;287(1):36–41.
[14] Ringel RL, Kahane JC, Hillsamer PJ, Lee AS, Badylak SF. The application of tissue engineering procedures to repair the larynx. J Speech Lang Hear Res 2006;49(1):194–208.
[15] Nieponice A, Gilbert TW, Badylak SF. Reinforcement of esophageal anastomoses with an extracellular matrix scaffold in a canine model. Ann Thorac Surg 2006;82(6):2050–8.
[16] Kochupura PV, Azeloglu EU, Kelly DJ, Doronin SV, Badylak SF, Krukenkamp IB, et al. Tissue-engineered myocardial patch derived from extracellular matrix provides regional mechanical function. Circulation 2005;112(Suppl. 9):I144–9.
[17] Voytik-Harbin SL, Brightman AO, Waisner BZ, Robinson JP, Lamar CH. Small intestinal submucosa: a tissue-derived extracellular matrix that promotes tissue-specific growth and differentiation of cells in vitro. Tissue Eng 1998;4(2):157–74.
[18] Reddy GK, Enwemeka CS. A simplified method for the analysis of hydroxyproline in biological tissues. Clin Biochem 1996;29(3):225–9.
[19] Gelman RA, Williams BR, Piez KA. Collagen fibril formation. Evidence for a multistep process. J Biol Chem 1979;254(1):180–6.
[20] Ray JL, Leach R, Herbert JM, Benson M. Isolation of vascular smooth muscle cells from a single murine aorta. Methods Cell Sci 2001;23(4):185–8.
[21] Birk DE, Silver FH. Collagen fibrillogenesis in vitro: comparison of types I, II, and III. Arch Biochem Biophys 1984;235(1):178–85.
[22] Grant DS, Leblond CP, Kleinman HK, Inoue S, Hassell JR. The incubation of laminin, collagen IV, and heparan sulfate proteoglycan at 35 degrees C yields basement membrane-like structures. J Cell Biol 1989;108(4):1567–74.
[23] Birk DE, Fitch JM, Babiarz JP, Doane KJ, Linsenmayer TF. Collagen fibrillogenesis in vitro: interaction of types I and V collagen regulates fibril diameter. J Cell Sci 1990;95(Pt 4):649–57.
[24] Brightman AO, Rajwa BP, Sturgis JE, McCallister ME, Robinson JP, Voytik-Harbin SL. Time-lapse confocal reflection microscopy of collagen fibrillogenesis and extracellular matrix assembly in vitro. Biopolymers 2000;54(3):222–34.
[25] Pins GD, Christiansen DL, Patel R, Silver FH. Self-assembly of collagen fibers. Influence of fibrillar alignment and decorin on mechanical properties. Biophys J 1997;73(4):2164–72.
[26] Ghosh K, Pan Z, Guan E, Ge S, Liu Y, Nakamura T, et al. Cell adaptation to a physiologically relevant ECM mimic with different viscoelastic properties. Biomaterials 2007;28(4):671–9.
[27] Chan RW, Titze IR. Viscosities of implantable biomaterials in vocal fold augmentation surgery. Laryngoscope 1998;108(5):725–31.
[28] Chan RW, Titze IR. Hyaluronic acid (with fibronectin) as a bioimplant for the vocal fold mucosa. Laryngoscope 1999;109(7 Pt 1):1142–9.
[29] Klemuk SA, Titze IR. Viscoelastic properties of three vocal-fold injectable biomaterials at low audio frequencies. Laryngoscope 2004;114(9):1597–603.
[30] Brown D, Maclellan W, Laks H, Dunn J, Wu B, Beygui R. Analysis of oxygen transport in a diffusion-limited model of engineered heart tissue. Biotechnol Bioeng 2006;97(4):962–75.
[31] Davis BH, Schroeder T, Yarmolenko PS, Guilak F, Dewhirst MW, Taylor DA. An in vitro system to evaluate the effects of ischemia on survival of cells used for cell therapy. Ann Biomed Eng 2007;97(8):1414–24.